

## MORPHOSTRUCTURAL ANALYSIS OF AN ALPINE DEBRIS FLOWS CATCHMENT: IMPLICATION FOR DEBRIS SUPPLY

A. LOYE<sup>(\*)</sup>, M. JABOYEDOFF<sup>(\*)</sup>, A. PEDRAZZINI<sup>(\*)</sup>, J. THEULE<sup>(\*\*)</sup>,  
F. LIÉBAULT<sup>(\*\*)</sup> & R. METZGER<sup>(\*)</sup>

<sup>(\*)</sup>Institute of Geomatics and Risk Analysis, University of Lausanne, Switzerland

<sup>(\*\*)</sup>Cemagref, Unité de Recherche Erosion Torrentielle, Neige et Avalanches, Grenoble, France

### ABSTRACT

Rock slope instabilities are implicitly linked to the supply of sediment and debris recharging channels prone to debris flow. Hence, the incorporation of bedrock structure and terrain morphology can be relevant in the analysis of sediment budget and debris flow hazard assessment. Here, the mode of debris production of the Manival catchment (northern French Alps) is documented by the study of its morphostructural aspects extracted from high resolution DEM. Terrain implication in the process of debris supply is evaluated by: a) A systematic classification of the major morphological units based on the slope gradient that enables a spatial analysis of zones of debris production and deposition. b) A detailed structural analysis performed on DEM in order to identify potential unstable slopes. c) An analysis of the gullies orientation that informs in term of structural control of the sources zones. d) Localisation of high density joints sets that document about whether sources of continuous debris production are controlled by the structural setting of the catchment. These DEM-based indicators can be used as proxies for assessing the influences of the current topography and enable to quantify a degree of susceptibility to mass wasting and hillslope erosion activity. This present contribution suggests some directions for characterizing sediment flux dynamic in small alpine catchment.

**KEY WORDS:** *Sediment budget, Erosion, Structural control,*

*Debris flow hazard assessment on DEM*

### INTRODUCTION

Debris flows transport large amounts of sediment out of the watershed over geological time scale. The size of debris/alluvial fans accumulated along valleys margins attests of the intensity of hillslope processes. From cursory field observation, erosion processes leading to debris supply recharging channels seems to be implicitly linked to the geomorphic and geostructural conditions prevailing at the source areas (cliffs and bedrock basin). Recent investigations have demonstrated that bedrock landslides and collapse of cliff faces by rockfall are a first order control of hillslope erosion rate (e.g. DENSMORE *et alii*, 1997; SCHRODER & BISHOP, 1998; HOVIUS *et alii*, 2006). Mass wasting production depends on one side from the lowering rate of local base level (e.g. DAVIS, 1899; HACK, 1960): the valley slopes steepen and become progressively unstable and collapse, involving not only the overlying sediment deposit but also the bedrock (BURBANK *et alii*, 1996). Rates and mechanism of debris production are controlled on the other side by the lithologic characteristics of the topography and the geology influencing the local state of stress (e.g. SAYCHIN *et alii*, 1998; ERISMANN & ABELE, 2001; CRUDEN, 2003). Historical investigation of small alpine catchment in the Swiss Alps have shown that periods of high debris flows magnitude and frequency result from intense rock-slides events or rock avalanches of  $Mm^3$  (EISBACHER

& CLAGUE, 1984; BARDOU *et alii*, 2003). Analyses of their magnitude have highlighted the coexistence of two types of processes describing the forming of debris flow volumes (HAEBERLI *et alii*, 1991; BARDOU & JABOYEDOFF, 2008):

*Continuous* debris supply linked to hillslope erosion processes in steady state; denudation behaves gradually and is related to weathering and rainfall intensity (climate-erosion relationship).

*By pulse*, through the occurrence of high magnitude (extraordinary) debris supply events (e.g. bedrock landslides) implying additional geological and structural predisposition.

Studies focusing on morphometric and topoclimate factors to enhance the understanding of the causal processes governing mass wasting and sediment flux are often limited by the small scales of investigation: at local scale, the topography, the tectonic setting and the climate are rather similar, whereas production rates of sediment and mechanism contributing to accumulate debris can be very heterogeneous throughout adjacent subcatchments. According to the fact that rock slope instabilities influence the supply and volume magnitude of debris, it seems relevant to incorporate the influence of bedrock structure as well as terrain morphology into assessment of basin scale sediment budget and debris flow hazard assessment.

The present study describes a way to document the mode of debris production by analysing the morphostructural aspects of a small alpine catchment prone to high magnitude debris flows and is illustrated by the Manival basin, a very active catchment of the Char treuse Massif (northern French Alps). The method bases on topographic elements that can be extracted from digital elevation model (DEM) and improved with geological maps. Erosion processes analysis is characterized in terms of process related morphology and slope failure susceptibility according to the general structural setting. These can be used as proxies for evaluating terrain implication in the process of debris supply or for preliminary assessing potential zones of erosion. This approach suggests a direction for further investigation on the geomorphostructural role contributing to characterize sediment flux dynamic in small alpine catchment

## METHODOLOGY

The topography of a catchment reflects the compounded influence of the mechanical properties of the

rocks, the depositional mode of the lithologies (bedding), their tectonic setting (folds, faults, joint sets) as well as the slope behaviour against mass wasting and erosion (LOCAT *et alii*, 2000). The major morphological units and their morphostructural pattern are now displayed in details through high resolution DEM. Thus, they can be identified, which enables to interpret the role of the major features of topography, such as the main structural sets shaping the slopes and the hillslope processes characteristic shapes (e.g. JABOYEDOFF *et alii*, 2004). The method introduces three DEM-based indicators that can provide information on the nature and mode of slope erosion activity.

There are:

- a classified slope steepness map.
- a map of susceptibility index to planar and wedge failures.
- a mean orientation of zones having high density sets of joints.

## CLASSIFIED MAP OF SLOPE STEEPNESS

The slope steepness influences shear stress intensity upon soil. Hence, the steepness of topography is directly involved in slopes stability, soil creeping and runoff rates. The slope morphology of a terrain is given by characteristic slope angles. The STRAHLER'S (1950) law of constancy of slopes states that slope morphology of a local topography tends to group prominently around a local mean slope angle values that are normally distributed with low dispersion. Hence, predominant sets of slope angle can be identified from DEM and related to the major morphological units forming the topography, such as torrential plain, debris-mantle slope deposits, cliffs (Fig. 2). Overlying this slope angle classification on a 3D shaded relief map enables a spatial analysis of process-related morphology, such as zones of debris production and deposition.

## POTENTIAL ROCK SLOPE INSTABILITIES DELINEATION

The significance of geologic structure on the slopes stability of bedrock has been demonstrated in the discipline of rock mechanics (e.g. TERZAGHI, 1962; HOEK & BRAY, 1981; SELBY, 1982). Studies that have focused on the structural control of erosion could show the link between structural geomorphic aspect and mass wasting (e.g. RAPP, 1960; GERBER & SCHEIDEGGER, 1973; SAYCHIN

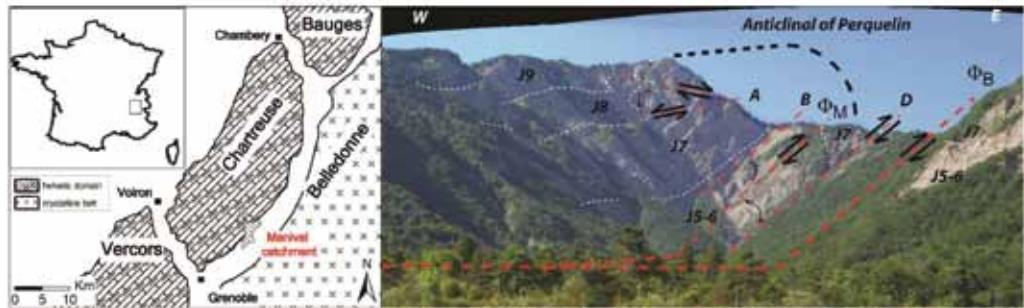


Fig. 1 - (left) Location of study area; the Manival catchment is displayed in light gray showing the impressive debris fan. (right) Photograph showing the upper Manival basin with the main lithologies and faults sets: J5-6: calcareous marl (upper Oxfordian), J7: marly-limestones (Sequanian), J8: stratified limestones interbedded with marls (Kimmeridgian), J9: massif limestones (Thitonian). A is an inverse compressive fault at the top. B and D are local minor inverse faults.  $\Phi_M$  Manival thrust,  $\Phi_B$  Baure thrust. (modified after [www.Geol-alp.com](http://www.Geol-alp.com) (Gidon 1991))

& GARDNER, 1983; GRIFFITHS *et alii*, 2004). Especially, the nature of discontinuity sets and their agencement according to the slope gradient of the topography influence more the stability of a rock slope than the intrinsic properties of an intact rock mass (e.g. NORRISH & WILLIS, 1996; ROULLER *et alii*, 1997; HANTZ *et alii*, 2003). In the same way, tectonic deformation such as fold position and relief geometry must be taken into account when considering rock slope stability (COE & HARP, 2007). In order to analyse whether this structural geometry contributes to slopes instability and gullies formation across the catchment, the major discontinuity sets are identified based on the analysis of the discontinuity surface contained in the topography. Potential unstable slopes and their mode of failure can be then localized in the catchment by performing a kinematic analysis. This enables to spatially illustrate where the topography in relation with the presence of discontinuities is a primary mode of potential slope mass instability.

#### STRUCTURAL CONTROL DESCRIPTORS

The influence of the discontinuity pattern on the current morphology of the catchment can be assessed using (SCHEIDEGGER, 1980; BEAVIS, 2000):

The maximum frequency orientation of the gullies.

The orientation of the maximum frequency of discontinuities.

These can inform not only in term of structural control of the cliffs and gullies, but enable to document whether sources zones of continuous debris and screes production are controlled by the structural setting of the catchment

#### IMPLICATION TO DEBRIS SUPPLY

The degree of susceptibility to slope instabilities can be quantified by its number of detected failure mechanism per surface area. The density of failure mechanism can be weighted by an assessment of its factor of safety. This enables to emphasize potential unstable zones in comparison to potential stable ones. When the topography shows a clear structural control of its morphology, zones of continuous debris supply can be delineated by assuming that sediment production should be located where the density of joints sets is more important. A susceptibility index of debris production can be then deduced by combining the zones of susceptibility to slope failures with the ones having a high density of joints and limited to a specific morphological unit.

#### STUDY AREA

The Manival catchment (Fig. 1 left) is a tributary to the Grésivaudan Valley located in the eastern border of the Chartreuse Massif, about 20 km north-east from the town of Grenoble (France). The Chartreuse mountain range belongs to the northern subalpine domain (or helvetic), that corresponds to the mesozoic cover of the external alpine crystalline belt. This massif has formed in an alternation of marls and limestone ranging from the upper Jurassic to early Cretaceous age and embedded in layers of decimetric to metric thickness. It displays a structure of inclined folds from Miocene age containing important and continuous overthrust faults in response to the NW-SE crustal shortening during the Alpine orogene (Gidon, 1991).

The erosion, especially in the eastern part of the massif, has since then deeply entrenched the folds, leaving a dissected relief with steep cliff faces.

The Manival catchment (Fig. 1 right) has developed in the most southeastern anticline of the massif, building one of the largest alluvial fan surfaces from the western Alps made of torrential debris. The valley covers an area of 3.7 km<sup>2</sup> from the top (1738 m) to the apex of the alluvial fan. The high ridge and peaks of the basin are made of massif (Tithonian) to stratified limestones interbedded in its lower parts by layers of marls (Kimmeridgian). Depending on the marls thickness, they can form well-defined escarpments. The mid-elevation slopes are generally made of marly limestone from the so-called Sequanian (Oxfordian-Kimmeridgian border). Those layers display another face of cliffs. The lower part of the catchment is made of calcareous marls of metric beds, alternating with marls from the upper Oxfordian. In the down part of the catchment, they are mostly covered by slope deposits, but exhibit steep slopes in the upper basin, although they might be less resistant. The two valley sides correspond to the limbs of the anticline. The hinge zone is cut by a system of two major inverse faults that cut sidelong the axis of the valley. It results a higher elevation of the western limb and the east part is reversed, leading to an inclined fold. Other minor faults exist. All those faults, as the lithologies, have probably played a major role in the impressive headward entrenchment depth of the catchment. Today, the erosion is still very active, but concentrated essentially in the upper catchment, at the bedrock basin displaying steep cliff walls. Steep slope gradient coupled with a very low vegetation cover and low permeability induce an important runoff as a response to heavy rainstorms that occur regularly up there due to enhanced convective cells. This is also responsible for an important bedload transport, erosion of screes covered slopes along the channel, interfluvial hillslope transport of sediment and initiation of debris flows. The middle and down part of the watershed, although quite steep as well, is well vegetalized. Their contribution in term of erosion activity must be therefore reduced.

## DATA PROCESSING

The study was conducted with a 1m cell size DEM derived from airborne LiDAR survey of the entire catchment operated in 2009.

## SLOPE STEEPNESS ANALYSIS

The slope angles map were created using a matrix of 3x3 DEM cells (BURROUGH & McDONNELL, 1997) and classified in steps of 1°. The frequency of occurrence of each class of slope angle was normalized considering their real surface. The slope angle frequency distribution (SAFD) was decomposed into several normal distributions, where the sum of those normal curves fits the SAFD (Fig. 2). This was processed using the freeware HistoFit (LOYE *et alii*, 2009), an Excel<sup>®</sup>-based application that computes the most-likely normal curves in an iterative way until their sum fits at best a target function represented here by a SAFD. The fitting process is done by minimizing the standard error using optimisation procedures of the Excel solver. The initial values are defined according to the shape of the SAFD, where local maximum and minimum can be identified visually along the curvature of the SAFD. The sets of slope steepness representing a morphological unit are delimited according to the slope angle where a normal distribution becomes dominant over the others. In example in fig. 2, the threshold for the cliffs is over 47°.

Morphostructural analysis and kinematic analysis

The major discontinuity sets of the catchment were identified based on the discontinuity surface of the 3D topographic analysis performed with the software Coltop 3D (JABOYEDOFF *et alii*, 2007). Coltop 3D enables an analysis of the topography by representing the dip and dip direction of the slopes of a DEM with a unique colour code, the Hue saturation intensity system (HIS). The topography is displayed as a 3D shaded relief and the colour code is ranged in value of a Schmidt Lambert projection. Considering that

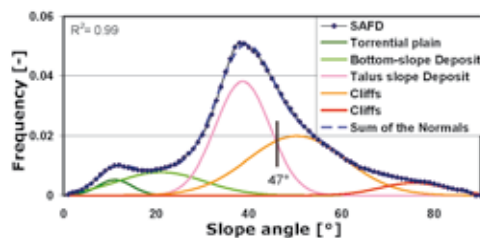


Fig. 2 - Slope angle frequency distribution (SAFD) of the Manival catchment and decomposition in major morphological units (displayed in fig. 3); 47° is a threshold above which the slopes can be considered as cliffs faces

Type	FS	Parameters
Planar	$\tan(\alpha) / \tan(\beta)$	$\Phi = 30^\circ$
		$\beta = \text{dip of the sliding plane}$
Wedge	$k \cdot \tan(\alpha) / \tan(\beta_w)$	$\Phi = 30^\circ$ ; $k = \text{wedge factor}$
		$\beta_w = \text{plunge of the wedge axe}$

Tab. 1 - Factor of safety (FS) computation (NORRISH & WILLIE, 1996)

Discontinuity sets	Coltop 3D data		
	Dip direction	Dip	Variability ( $2\sigma$ )
J1	155°	64°	16
J2	187°	53°	14
J3	220°	62°	16
J4	261°	50°	15
J5	350°	60°	19
J6	044°	47°	14
J7	106°	74°	17

Tab. 2 - Threshold slope angles defining Morphological units

DEMs display surface features that can reflect several structural information, Coltop 3D enables a detailed investigation of the discontinuity sets shaping the rock slope of a catchment. When such analysis is based on airborne DEM acquisition, slopes with overhanging structures are not detected. They can however be identified in some other parts of the slope where they outcrop. The structural setting was then compared with field observation and terrestrial laser scanner data.

The identified discontinuity sets were compared with the entire topography using the software Matterocking (JABOYEDOFF *et alii*, 2004). This GIS tool enables to assess potential planar and wedge sliding area on DEM and gives the average number of failure mechanism per DEM cell, according to a given spacing between discontinuities. All discontinuities were processed according to their mean azimuth and dip. An arbitrary spacing of 1 m (corresponding to the DEM resolution) was assumed for all discontinuity sets. Wedges with plunge axes  $<20^\circ$  were considered as marginally potential and not further considered.

**STRUCTURAL CONTROL ASSESSMENT**

The distribution of the gullies geometries was extracted from the virtual rivers of the DEM. Flow paths were determined by the D8 algorithm (O'CALLAGHAN *et alii*, 1984) considering a contributing area of 5000

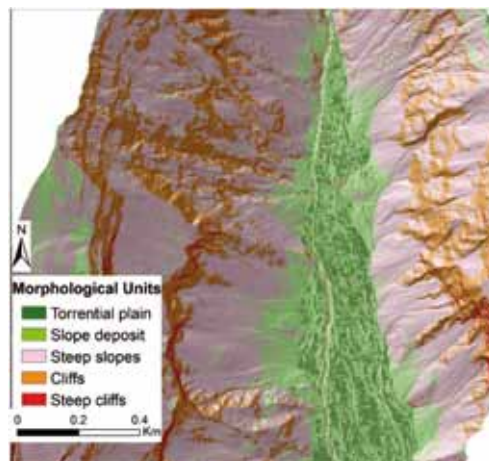


Fig. 3 - Classified slope steepness map highlighting the major morphological units. Note the rugged torrential plain, the debris cones on the east side and the slope bottom deposit on the west side of the valley

m<sup>2</sup>. However, only flow paths lying above the torrential plain were kept for the analysis, as below they are not structurally controlled. The frequency of the gullies geometry was plotted in a stereonet corresponding to a histogram in 3D and the density stereonet of the discontinuity sets were computed with the HUDSON & PRIEST'S (1983) method considering a similar spacing for all sets. The distribution of the discontinuity density was classified in two classes, the threshold being the density value reaching 95% of the cumulative distribution. The weighted density of potential slope failures was defined by dividing the average number of intersections per DEM cell by its factor of safety based on the limit equilibrium analysis (tab. 1), assuming that sliding is resisted only by friction similar for all planes. In this study case, the weighted relative density index for both planar and wedge are classified in three sets were their cumulative distribution defined at the 68-quantile, respectively 95-quantile.

**RESULTS AND ANALYSIS**

**SLOPE ANGLE FREQUENCY DISTRIBUTION ANALYSIS**

The decomposition of the SAFD with the tool Histofit was achieved using 5 normal distributions (Fig. 2). Several initial values were tested, which yield to similar normal curves pattern for most of the cases. The sum of the normal curves reproduces the SAFD of the Manival topography with a coefficient of determination

Discontinuity sets	Coltop 3D data		
	Dip direction	Dip	Variability ( $2\sigma$ )
J1	155°	64°	16
J2	187°	53°	14
J3	220°	62°	16
J4	261°	50°	15
J5	350°	60°	19
J6	044°	47°	14
J7	106°	74°	17

Tab. 3 - Discontinuity sets for the Manival catchment

close to 1, meaning that the morphology is clearly constrained. Threshold slope angles delimiting the sets of slopes steepness are summarized in table 2. Overlying this classified slope steepness map with the shaded relief map (Fig. 3) enables to identify 4 morphological units:

The lowest set corresponds to the torrential plain. This range of slope steepness delineates the torrential plain full of sediment deposited throughout the valley bottom.

The 2<sup>nd</sup> set of steepness displays the debris cones deposited at the mouth of the tributary gullies and the bottom-slope deposit cover located at the margin of the valley bottom.

The 3<sup>rd</sup> range of steepness covers all talus slope deposits and outcropping bedrock slopes lightly covered with vegetation. They are located both downslope and upslope from cliff faces.

The steepest sets delineate the cliffs, rocky escarpment and the steep bedrock slopes. Two sets of cliffs were input for a better fitting of the SAFD.

**MORPHOSTRUCTURAL ANALYSIS**

The Coltop 3D analysis has identified 7 major topographic orientations (Fig. 4) spatially well distributed and continuously present in the Manival catchment (Fig. 5). Four discontinuity sets (J5, J6, J7 and J1) are mainly encountered in the west side of the valley, whereas J1 is a well-defined discontinuity encountered on both sides to the top of the catchment. J5 possesses a more dispersed orientation and develops exclusively in the deep vertical gullies of the western slopes. It is possible that J5 represents only a steep geomorphic features influenced by gully activity, but may not belongs to J6, for example, which is very constant with its orientation ranging of  $\pm 14$  around its mean value. The east side of the catchment are shaped

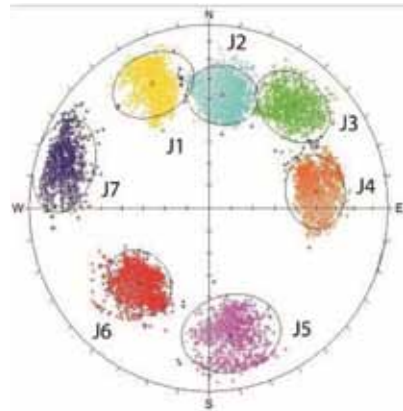


Fig. 4 - Discontinuity sets extracted from DEM using COLTOP 3D. The black circle represents the variability ( $2\sigma$ ). Values are given in Tab 3

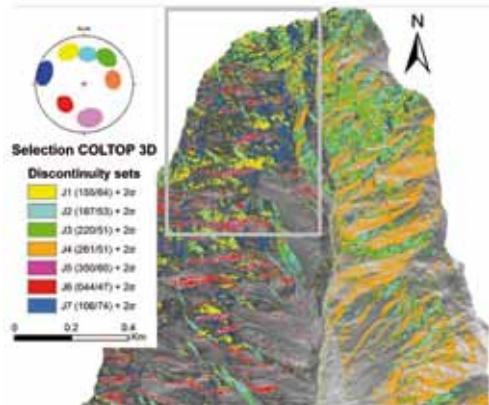


Fig. 5 - Discontinuity sets extracted from DEM using COLTOP 3D. The geometry of each set is given with its variability of  $2\sigma$  (see Tab. 3)

by J1 and J4. J7 on the west and J2 and J3 on the east part define rather clear geomorphic features as they displays most of the cliffs facing the valley bottom of the entire catchment. The bedding is gently dipping in the slope (anaclinal) in most of the catchment.

Bedding field measurements give out a mean orientation around  $270^\circ/35^\circ$  for the west slopes and around  $100^\circ/45^\circ$  for the east slope down the valley but becomes much more variable in the upper catchment and around the local zones of deformation. But as the bedding planes could not be well identified with COLTOP 3D, they were not taken into account in this study. They are however important in the west slopes as they can induce toppling (not yet processed in this study). The structural scheme is illustrated on pictures (Fig. 6).

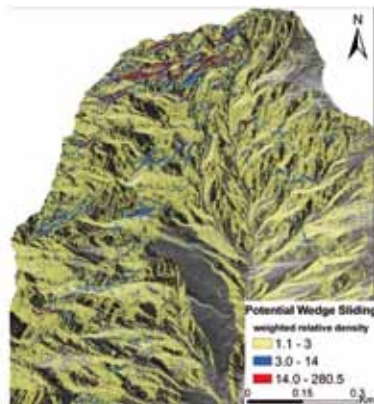
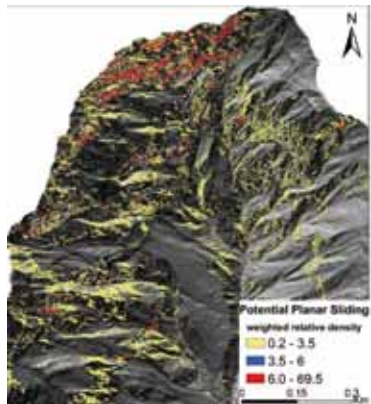


Fig. 7 - Classes of susceptibility to planar (left) and (right) wedge sliding according to their weighted relative density



Fig. 6 - Field illustration of the structural scheme detected on DEM. The location of the photograph is displayed in fig. 5

POTENTIAL FAILURE MECHANISM AND LOCALISATION

The map of potential planar sliding shows a high susceptibility for the steep slopes facing southeast, which are concentrated mainly on the top central part (Fig. 7 left). These imply joints set J1, J2 and J3 predominantly. On the west side of the valley, gullies flanks facing north are exposed to planar failures. The slope stability seems to be controlled by J6 in this area. On the east side, they concentrate on the steep slopes only. Zones of potential wedges are widespread in the catchment according to the joints sets of this study (Fig. 7 right). However, its weighted relative density is very low for most of the catchment. High susceptibility to wedge sliding is encountered mainly in the steep slopes facing S-SE, but not only. Several steep enough slopes, like the ones surrounding the major gullies on the west side display a relatively middle high susceptibility. They are controlled by wedges set configuration J5^J6, J5^J7 and J6^J7

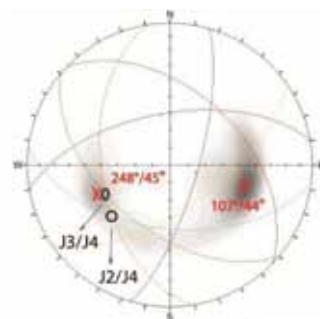


Fig. 8 - Frequency stereonet of gullies orientation (picks red cross) and comparison with the sets of discontinuities

STRUCTURAL CONTROL DESCRIPTORS INTERPRETATION

The frequency stereonet of the gullies orientations (Fig. 8) gives two major poles. The pick 107°/44° corresponds to the mean dip/dip direction of the west side catchment flow paths. Comparing this pick value with the geometry of the discontinuities identified on these slopes shows that the gullies follow rather the slope gradient than one preferential discontinuity configuration. In the contrary, the pick value 248°/45° is linked to the east side and suggests that gullies are strongly influenced by J4 and its wedges formed with J3 (and J2 accessory). This value is slightly different from the greatest slope gradient, implying a potential structural control of the flow paths.

The maximum density of discontinuities assuming an identical mean spacing for all joints sets leads to an orientation of about 200°/70° with certain variability of 20° (Fig. 9). Considering that J1 and J6 are very persistent over the all massif and that J3^J4 controls the topography of the east side, the mean spacing of these three discontinuities were doubled. The

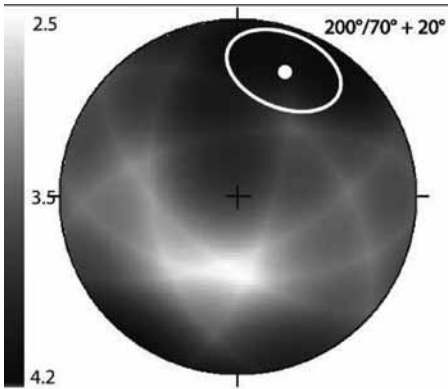


Fig. 9 - Geometry of the maximum frequency of the discontinuity pattern of manival catchment

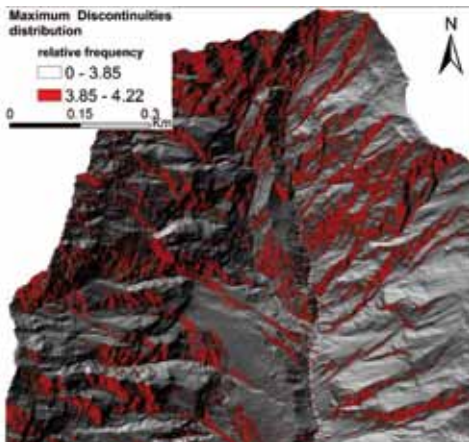


Fig. 10 - Map of the zones having a high density sets of joints

orientation of the maximum density is then situated around  $205^{\circ}/64^{\circ}$ , relatively closed to the previous value. Zones of high density joints sets are oriented S-SW and follow most of the cliffs surrounding tributary gullies on both sides of the valley (Fig. 10).

## DISCUSSION

The morphological units extracted from the SAFD analysis provides a systematic approach for delineating debris sources areas such as the cliffs and zones of deposition and remobilisation such as slopes deposit and alluvial plain. The threshold slope angle above which the slopes can be considered as cliff faces and outcropping bedrock is  $47^{\circ}$ . This is comparable to what has been obtained in the Helvetic and Ultrahelveti Swiss Alps (LOYE *et alii*, 2009). Combining this slope angles classification with field observation

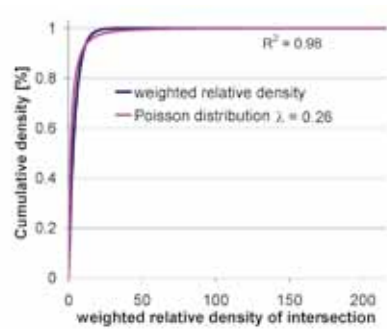


Fig. 11 - Cumulative distribution of the weighted density of potential wedge sliding intersection (shown in fig. 7) and the fitted Poisson distribution

of the morphology can inform about the mode of debris production and transportation. The surface of the torrential plain is rugged (Fig. 3), showing several remnant channel beds. This high amount of old channels can attest of high magnitude debris flow events in order to change the course of the main channel. The mean steepness of the torrential plain is  $11^{\circ}$  (20%), which corresponds to the mean angle of repose of granular debris flow type (RICKENMANN, 1995). The *bottom-slope deposit* morphological unit can be separated in two types according to their form and their clear break of slope angle at the interface with the torrential plain (Fig. 3):

1. Cone-shaped deposits at the mouth of ephemeral gullies; their relative steep slope of deposition suggests a rockfall-dominant type of deposit. Water-dominated flow and debris flow fans are usually less steep, because they are composed of less thicker and coarser material. These cones are entrenched by ephemeral channels.
2. Sediment deposit at the toe of the talus slopes, gently flatten footslopes made of rock fragments and covered with mature vegetation suggest progressive deposition of mode *wash slope*.

The upper catchment displays no cone-shaped or bottom-slope deposit at the toe of gullies and cliffs showing an absence of long term mass wasting deposit coming from the sides of the valley and high connectivity of the entire upper catchment to transport debris away. Debris flow frequency seems therefore to be supply-limited.

The 3D analysis of the major topographic orientation performed with Coltop 3D enables to identify the major discontinuities structuring the topography

of the catchment. Representing the pattern of discontinuities on the shaded relief map shows that they cover about 25% of the computed horizontal surface and are spatially well distributed, meaning that the topography of the catchment is rather shaped by this structural setting. J1 and J6 are clearly involved in the shape of large tributary gullies. J1 seems to be very persistent, as it is found on both side of the valley. J4 seems to control large slope surfaces of the east side of the valley and is cut laterally by J1 and J2 to form a succession (en echelon) of small gullies and v-shape geomorphic features. J3 and J7 display clear and continuous geomorphic features as they draw most of the cliffs facing the valley bottom. In the top central part, J1 and J7 control the rock walls, whereas J4 and J6 clearly control the morphology in a wedge like configuration and confirm that they are true discontinuity sets. Photograph analysis show that J4 represents here the bedding plane but this is not the case anymore as it goes away from the top central part and on the side of the valley. The weighted relative density of joints that fulfils the conditions for potential planar and wedge failure show that the central top part of the catchment is well exposed to slope instabilities. They are produced on joint sets J1, J2 and J3. Potential planar sliding zones follow the south flanks of the large gullies situated on the western part and can be a mode of debris supply into the channels. High weighted relative density of wedges is located principally (but not only) in the slope facing S-SE as is it the case for planar sliding. Cliffs surrounding gullies with such an orientation are susceptible to experiment high debris supply. In this study, the weighted relative density of both failure mechanisms could be modelled by a Poisson distribution (Fig. 11). The widespread potential wedge sliding demonstrates that the present discontinuities sets play an important role in the slope stability of the catchment, even though most of the zones have a low susceptibility. This can be partly explained by the wedge-like configuration of the east and central part of the topography mentioned above. The influence of discontinuities, such as faults and fractures, can be underlined by the frequency stereoplot of the gullies geometry. The gullies of the upper eastern catchment part are directed principally in the same direction of J4 and oriented within the wedges caused by J3^J4, showing a clear structural control. The western side is apparently not structurally controlled. Its great steep-

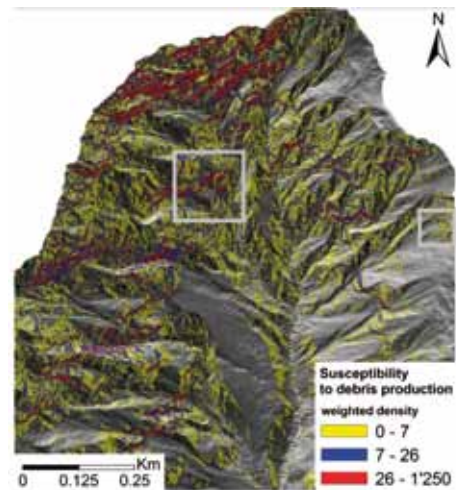


Fig. 12 - Map of susceptibility to debris production according to the combination of the three DEM-indicators processed in this study (yellow=low, blue = mid, red = high susceptibility)

ness may however bias the analysis, because the gullies are clearly chopped by J1 and J6.

The analysis of the maximum density of discontinuity reveals mean orientations defining steep slopes surfaces that are facing S-SW. They follow alongside the gullies particularly well and on both side of the catchment. Hence, production of continuous rockfall screes and debris must be located where the zones with high density of discontinuities are.

The susceptibility index of debris production is obtained by multiplying this apparent density of discontinuity with the weighted relative density of failure mechanism (sum of potential planar and wedge failures) (Fig. 12). This is classified in three sets (low, mid and high susceptibility) where the cumulative distribution defines the 50-quantile, respectively 75-quantile, as suggested by comparing the index with orthophotos and field observation (Fig. 13).

## CONCLUSION AND OUTLOOK

Observation and investigation on shaded high resolution DEM of the major morphological units delineated with the classified slope angle map enable to identify evidences of debris production and deposition such as rockfall deposit and debris flow activity. Sediment slopes accumulation in contact with channels and gullies can inform on the sediment supply dynamic. The DEM-based indicators devel-

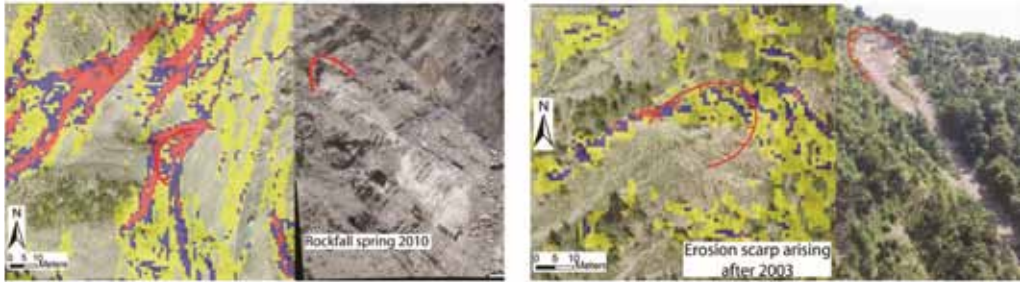


Fig. 13 - Two erosion scarps arising recently and supplying the channel with debris as field observation that enable to evaluate the DEM-indicators. (left) Close-up of fig. 12 displaying the susceptibility index to debris production on orthophoto (© IGN). (right) Field photographs taken in summer 2010

oped in this study can assess the influence of the morphostructural aspect on the current morphology of the catchment and enable to quantify a degree of susceptibility to mass wasting and hillslope erosion activity. Processes related to rock slope instability and continuous debris production are potentially distinguishable by assuming that continuous sediment supply must be located where high density joints sets are. All these affirmations must be verified with field measurements. The erosion activity of cliffs and gullies of the upper rock basin at Manival has been monitored periodically with terrestrial laser scanner

since 2009 and should provide volume and magnitude of sediment to quantitatively highlight the main geomorphic processes controlling the production of debris. So far, this approach was compared with aerial photo analysis and field observation only (Fig. 13), but first results are promising.

#### ACKNOWLEDGEMENTS

The first author would like to address his gratitude to M.-H. Derron and B. Matasci from the UNI Lausanne for their constructive comments and ideas during the development of this study.

#### REFERENCES

- BARDOU E., FOURNIER F. & SARTORI M. (2003) – *Paleofloods reconstruction on Illgraben torrent (Switzerland): a need for today frequency estimation*. Intern. Workshop on Paleofloods, Historical Data & Climate Variability: Application in Flood Risk Assessment, Barcelona.
- BARDOU E. & JABOYEDOFF M. (2008) – *Debris flows as a factor of hillslope evolution controlled by a continuous or a pulse process?* FROM: GALLAGHER K., JONES S. J. & WAINWRIGHT J. (eds) - *Landscape evolution: Denudation, Climate and Tectonic Over Different Time and Space Scales*. Geological Society, London, Special Publication, 296: 63-78.
- BEAVIS S. G. (2000) - *Structural controls on the orientation of erosion gullies in mid-western New South Wales, Australia*. *Geomorphology*, **33**: 59-72.
- BURBANK D.W., LELAND J., FIELDING E., ANDERSON, R.S. BROZOVIC, N., REID M.R. & DUNCAN, C. (1996) - *Bedrock incision, rock uplift and threshold hillslopes in the northwestern Himalayas*. *Nature*, **379**: 505–510.
- BURROUGH P. & McDONNELL R. A. (1997) - *Principles of Geographical Information Systems*. Oxford University, 330 pp.
- COE J.A. & HARP E.L. (2007) – *Influence of tectonic fording on rockfall susceptibility*. American Fork Canyon, Utah, USA. *Nat-Hazards Earth Syst. Sci.*, **7**: 1-14.
- CRUDEN D.M. (2003) - *The shapes of cold, high mountains in sedimentary rocks*. *Geomorphology*, **55**: 249-261.
- DAVIS W.M. (1899) - *The geographical cycle*. *Geography Journal*, **14**: 481-504.
- DENSMORE A.L., ANDERSON R.S., McADOO B.G. AND. ELLIS M.A (1997) - *Hillslope evolution by bedrock landslides*. *Science*, **275**, 369-372.
- EISBACHER G.H. & CLAGUE J.J. (1984) – *Destructive mass movement in high mountains: hazard & management*. *Geol. Survey of Canada*, **84**: 16.
- ERISMANN T. H. & ABELE G. (2001) - *Dynamics of rockslides and rockfalls*. Springer, Berlin, 316, 2001.
- GERBER E. & SCHEIDEGGER A.E. (1973) - *Erosion and Stress-induced features of steep slopes*. *Z. Geomorphol. N.F., Suppl. Band* **18**: 38-49.

- GIDON M. (1991) - *Géologie de la Chartreuse - Sentiers de la Chartreuse*. Circuit de la Dent de Crolles. Association "A la découverte du Patrimoine de Chartreuse", publ. 1d, 1<sup>o</sup> éd., 20 p., 9 fig., www.Geol-alp.com.
- GRIFFITHS P.G. & WEBB R.H. (2004) - *Frequency and initiation of debris flows in Grand Canyon, Arizona*. J. Geophys. Res., 109, F04002.
- HACK J. T. (1960) - *Interpretation of erosional topography in humid temperate regions*. American Journal of Science, 258-A: 80-97.
- HAEBERLI W., RICKENMANN D. & RÖSSLU U. (1991) – *Murgänge, Ursacheanalyse der Hochwasser 1987*. Ergebnisse der Untersuchung. Mitt. No. 14. Landeshydrologie und –geologie, Bern.
- HANTZ D., VENGEON J. M. & DUSSAUGE-PEISSER C. (2003) - *An historical, geomechanical and probabilistic approach to rockfall hazard assessment*. NHESS, 3: 693-701.
- HOEK E. & BRAY J.W. (1981) - *Rock Slope Engineering*. The Institution of Mining and Metallurgy, London. 525 pp.
- HUVIUS N. & STARK C.P. (2006) - *Landslide-driven erosion and topographic evolution of active mountain belts*. In: EVANS S.G. et alii (Eds.). *Landslides from massive rock slope failure: 573-590*, Springer.
- HUDSON J.A. & PRIEST S.D. (1983) - *Discontinuity frequency in rock masses*. International Journal of Rock Mechanics and Mining Sciences & Geomechanics Abstracts, 20: 73–89.
- JABOYEDOFF M. (2002) - *Matterocking v 2.0: A program for detecting rockslide instabilities* (available on www.crealp.ch).
- JABOYEDOFF M., BAILLIFARD F., PHILIPPOSIAN F. & ROUILLER J.-D. (2004) - *Assessing fracture occurrence using "weighted fracturing density": a step towards estimatin rock instability hazard*. NHESS, 4: 83-93.
- JABOYEDOFF M., MEITZGER R., OPPIKOFER T., COUTURE R., DERRON M.-H., LOCAT J. & TURMEL D. (2007) - *New insight techniques to analyze rock-slope relief using DEM and 3D-imaging cloud points: COLTOP-3D software*. In: EBERHARDT E., STEAD D. & MORRISON T.: *Rock mechanics (2007, eds) - Meeting Society's Challenges and demands (Vol. 2)*, Taylor & Francis: 61-68.
- LOCAT J., LEROUEIL S. & PICARELLI L. (2000) - *Some considerations on the role of geological history on slope stability and estimation of minimum apparent cohesion of rock mass*. In: BROMHEAD E., DIXON N. & IBSEN M.L. (eds) - *Landslides in research, theory and practice*. 8<sup>th</sup> International Symposium on Landslides in Cardiff: 935-942.
- LOYE A., JABOYEDOFF M. & PEDRAZZINI A. (2009) - *Identification of potential rockfall source areas at a regional scale using a DEM-based geomorphometric analysis*. Nat. Hazards Earth Syst. Sci., 9: 1643-1653.
- NORRISH N.I. & WYLLIE D.C. (1996) - *Rock slope stability analysis*. Transportation Research Board. Special Report, Serial. Published in Washington D. C., 247, 509-513.
- O'CALLAGHAN J.F. & MARK D.M. (1984) - *The extraction of drainage networks from digital elevation data*. Computer Vision, Graphics, and Image Processing 28: 323-344.
- RAPP A. (1960) - *Talus slopes and Mountain Walls at Tempelfjorden, Spitsbergen*. Not. Polarins. Skr. 119, 96 pp.
- RICKENMANN D. (1995) - *Beurteilung von Murgängen*. Schweizer Ingenieur und Architekt, 48: 1004-1008.
- ROUILLER J.-D., JABOYEDOFF M., MARRO C. & PHILIPPOSIAN, F. (1997) - *Matterock: méthodologie d'étude d'instabilités de falaise et d'appréciation du danger*. Publications de la Soc. Suisse de Méc. Sols et roches, 135: 13-16.
- SAUCHYN D. J. & GARDNER J. S. (1983) - *Morphometry of open rock basins, Kananaskis area*. Canadian Rocky Mountains. Can. J. Earth Sci., 20: 409-419.
- SAUCHYN D.J., CRUDEN D.M. & HU X.Q. (1998) – *Structural control of the morphometry of open rock basins, Kananaski region, Canadian Rocky Mountains*. Geomorphology, 22: 313-324.
- SCHEIDEGGER E. A. (1980) - *Alpine joints and valleys in the Neotectonic stress-field*. Rock Mech. Suppl., 9: 109-124.
- SHRODER J. F. & BISHOP M. P. (1998) - *Mass movement in the Himalaya: new insights and research directions*. Geomorphology 26: 13-35.
- STRAHLER A.N. (1950) - *Equilibrium theory of erosional slopes approached by frequency distribution analysis*. American Journal of Science, 248: 673-696, 800-814.
- SELBY M.J. (1982) - *Controls on the stability and inclinations of hillslopes formed on hard rock*. Earth surface Processes and Landforms: 449-467.
- TERZAGHI K. (1962) - *Stability of slopes on hard unweathered rock*. Geotechnique, 12: 251-263.